JOURNAL OF INFORMATION SCIENCE AND ENGINEERING 25, 481-497 (2009)

A Novel Exemplar-Based Image Completion Model*

JI-YING WU AND QIU-QI RUAN
Institute of Information Science
Beijing Jiaotong University
Beijing, 100044 P.R. China

In this paper, a novel exemplar-based completion model which is used to remove objects from natural image and texture image is proposed. Firstly the model selects a dynamic size of exemplar based on the local texture information. Secondly, the filling order of exemplar is determined by a cross-isophote diffusion data item. The data item is the result of partial differential equation (PDE) which is derived based on the geometrical property. It considers the extent of edge, so it has a good linear structure preserving property. Thirdly, when processing the textured image, both color and gradient information is incorporated into the similarity function, and then the right texture patterns are preserved. Lastly, a gradient constrained total variation (TV) interpolation is used to reduce seams between exemplars in the completed image. Both theoretical analysis and experiments are given to demonstrate the performance of our model.

Keywords: image completion, exemplar-based model, partial differential equation (PDE), composite similarity function, removing seams

1. INTRODUCTION

Removing objects and restoring damaged image are important image processing tasks. Given an input image with selected target regions, both the geometrical property and color information should be propagated from the known parts of image into the target regions. However, the removed target region is selected by user, and then the completion procedure is executed automatically and seamlessly.

There are mainly three approaches related to image completion. The first one is image inpainting. The concept of image inpainting is proposed by Bertalmio in [1]. It uses an along isophote diffusion partial differential equation (PDE) to propagate the known image information into the target region. PDE updates a pixel's gray value based on the geometrical information in adjacent domain. It preserves the linear structure and smoothes region contour. When the target region is small, the visual perception of the generated image is good. PDE processes image only based on the local information, so when the target region is large or textured, the visual perception of the processed result is bad. PDE can not reconnect the linear structure in a large region and it can not restore texture patterns. There are many PDE-based inpainting models [2-5], and all of these models are suitable for completing small, non-textured target region.

Texture synthesis is another kind of image completion. It regenerates texture patterns in the target region. It aims at restoring texture pattern properly and seamlessly.

Received May 17, 2007; revised September 4, 2007; accepted September 28, 2007.
Communicated by H. Y. Mark Liao.
* This paper was partially supported by the National Natural Science Foundation of China under grants No. 60472033, No. 60672062; the National Grand Fundamental Research 973 Program of China under grant No. 2004CB318005; and the Technological Innovation Fund of Excellent Doctorial Candidate of Beijing Jiaotong University No. 48026.

The texture synthesis model uses variable neighborhood searching to preserve the entire texture pattern [6]. Graphcut approach is used to reduce seams between texture patches, and it generates ω-tile set to avoid highly repetitive patterns [7]. A non-parametric method based on Markov random field theory is introduced to preserve the local structure and produce a wide variety of textures [8]. The contrast enhancement is also used to generate image with a good visual perception [9]. Vector quantization is used to get a fast texture synthesis model [10]. The non-parametric model is extended to exemplar-based to accelerate the computing speed in [11]. All texture synthesis approaches process image based on the global information, and the entire texture pattern in image is resorted. They deal nothing with the local geometrical property, so they can not preserve the linear structures well in image. Texture synthesis is not suitable for geometrical image completion.

Efros proposed the exemplar-based texture synthesis model [11]. Bornard introduced this model into the geometrical natural image completion [12], and Perez proved that used in geometrical image completion this kind of model could generate a good result [13]. In exemplar-based image completion model, the basic unit of synthesis is a filling patch (exemplar) more than a single pixel. An exemplar is compared and copied during the completion procedure. Harrison determines the filling order by "textureness" of pixel [14], and the pixels which are highly constrained by neighborhood pixels have higher filling priorities. Although this intent is good, strong linear structures can not be properly preserved. The method proposed by Drori "iteratively approximates the unknown region and fills in the image by adaptive fragments" [15]. It uses an inverse alpha matte as the confidence map to determine the traversal order. This method is time-consuming and it can not often generate good result. Jian *et al.* introduced an image completion model with structure propagation [16]. User should mark the linear structure in the target region firstly and then the image patch is copied along the prescribed direction. This model generates good image but it needs user's interaction. Criminisi proposed an exemplar-based image completion model which determined the filling order under the constraint of PDE-based data item [17]. The exemplar which is along a linear structure has a higher filling priority, and the geometrical property in the completed image is preserved. Another cross-isophote diffused PDE is used in the completion model which has a better structure preserving property [18, 19].

In this paper, a novel exemplar-based image completion model is proposed. The novel model follows the basic conception in [17], and it does not need user's interaction. When the removing or restoring target region is selected, it processes image automatically. The whole image domain is Ω, the removing or restoring target region domain is D, and image information in D^c ($\Omega - D$) is known; the basic unit of synthesis is the exemplar Ψ. Image completion generates image information in D according to the information in D^c, and the whole exemplar Ψ is copied every time. The novel model proposed in this paper uses a dynamic size of exemplar restore the target region, and the size depends on the local texture information. The model uses a cross-isophote diffusion PDE constrain the filling order of exemplar. When there are different kinds of texture patterns in image, the linear structure is restored firstly, and then the proper exemplar could be found and copied. The difference between exemplars is used to weigh the exemplar similarity, and the color distance is often adopted. When a textured image is processed, the geometrical difference between exemplars should be considered. So a composite similarity function

which is determined by both the color and gradient information is used to compute the exemplar similarity. Then the proper textured exemplar could be found in the textured image completion. The exemplar-based model induces severe seams. When an exemplar is copied into the target region, a divergence constrained total variation (TV) interpolation is executed to reduce seams between exemplars and then the completed result is a smooth image.

The main contribution of our model is:

- It can properly complete image when there are different kinds of texture patterns;
- It has a good linear structure preserving property;
- It can find the most similar exemplar in the textured image based on both color and gradient information;
- There are no seams between exemplars in the completed image;
- It uses a half-point numerical difference scheme to implement the data item.

There is another issue relating to image completion. The completion result greatly relies on the selected target region. For the same original image, if the target regions are selected differently, the results generated by the same completion model are different. This is also proved experimentally in this paper. Like other exemplar-based model, our model finds the most similar exemplar according to the known image information. If there is no similar exemplar, the visual perception of the completed result is not good. To overcome this drawback, a training set containing more kinds of texture patterns can be used, and the exemplar is selected in this training set.

2. THE NOVEL MODEL

2.1 Overview of the Novel Model

The basic conception of our model is copying information from the source exemplar in the known parts of image into the target region. The selection of the source exemplar is determined by similarity function. Similarity is computed by the difference between pixels in two exemplars. Detailed completion procedure of the model is shown in the block diagram in Fig. 1.

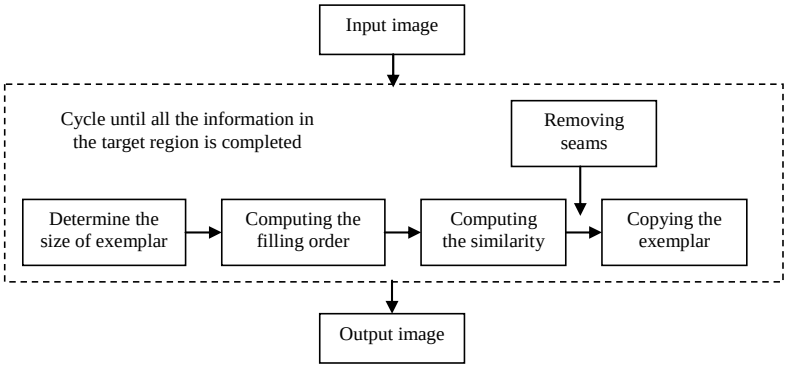

Fig. 1. The completion procedure of our model.

The input of the completion algorithm is an image which contains the masked target region D, and the output is a completed image with the region D filled.

2.2 Dynamic Size Exemplar

Since the basic unit of synthesis is exemplar, the exemplars in the target region are completed orderly. In conventional models, all the exemplars in the target region have a single fixed size. And then the filling order of these exemplars with the same size is determined. Generally, the size is chosen the same as that of the largest texture pattern to preserve more texture information in image [11-13]. There are some drawbacks if the exemplar is small, texture patterns are not thoroughly preserved; if it is too large, some tiny texture information will be lost. So in this paper, the size of each exemplar is dynamically determined. An initial size is assigned to all exemplars, and then the sizes of each exemplar are determined by the local textured property in exemplars, respectively. After determined the dynamic sizes of all exemplars, the filling orders of them are computed.

The distribution of the local texture patterns is periodic, and the color information is stochastic [20]. The statistical property of textureness in an exemplar is represented as

$$T(\mathbf{\Psi}) = \frac{\sum_{\xi \in \Psi} G(\xi - \xi_0) f(I(\xi) - \mu)}{N(\mathbf{\Psi})} \tag{1}$$

where $\mathbf{\Psi}$ is the exemplar, $T(\mathbf{\Psi})$ represents the statistical property of the textured information in $\mathbf{\Psi}$, $I(\xi)$ is the color value of pixel ξ in $\mathbf{\Psi}$, μ is the average color value of all pixels in $\mathbf{\Psi}$, f computes the color difference between isolated pixel and the average result of all pixels in $\mathbf{\Psi}$, ξ_0 is the central pixel, $N(\mathbf{\Psi})$ is the number of pixels in $\mathbf{\Psi}$, G is Gaussian function which is used to weigh the space difference between ξ and ξ_0. The algorithm used to determine the size of exemplar is shown in Fig. 2.

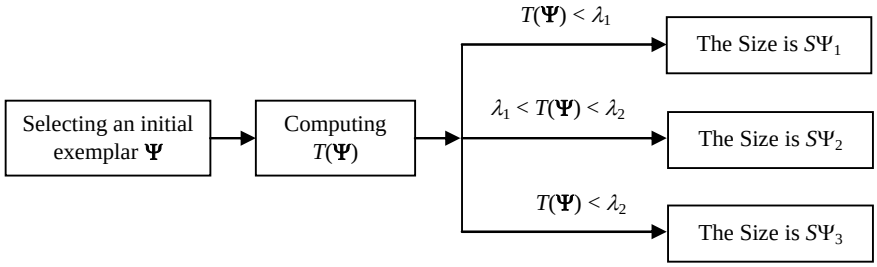

Fig. 2. The algorithm used to determine the size of exemplar.

In this algorithm, the input is an exemplar in the target region. An initial size of it is assigned. Used in image completion, the ordinary sizes of exemplars are 3×3, 4×4 and 5×5. In this paper, the initial sizes of all exemplars are assigned to be 4×4. The computed $T(\mathbf{\Psi})$ is then compared with textured thresholds λ_1, λ_2 ($\lambda_1 < \lambda_2$).The thresholds are determined experimentally and they are the variables which 30% and 60% computed

$T(\Psi)$ are smaller than, respectively. If the exemplar contains textured information, the difference between pixels in it is large. So the value of $f(I(\xi) - \mu)$ is large and $T(\Psi)$ is large. In Fig. 2, this situation is represented as $T(\Psi) > \lambda_2$. To preserve the entire textured information, the size of this exemplar should be large, and then the size is $S\Psi_3$ and $S\Psi_3 = 5 \times 5$. If the exemplar is non-textured, the difference between pixels is small, and then $T(\Psi)$ is small. The size of exemplar should be small to not copy error texture patterns into the target region. The size is $S\Psi_1$, and $S\Psi_1 = 3 \times 3$. Executing the algorithm described in Fig. 2, the value of $T(\Psi)$ is computed and then the proper size of exemplar is determined. The output of this algorithm is the image exemplar Ψ with a proper size.

2.3 Data Item Constrained Filling Order

In the conventional exemplar-based model, the filling order is onion-peel: the exemplar which contains more known information has a higher filling priority [8, 11]. The completion procedure takes place from the outmost to the center part. Used for texture synthesis, the exemplar-based model using onion-peel order could generate a good result, since texture synthesis replicates a single kind of texture pattern [8]. For image completion, this filling order is not suitable. In natural image, there are different kinds of texture patterns separated by linear structures. The completion model should preserve linear structures and find proper filling exemplars. Following the basic conception in [17], the filling order is determined by the product of confidence item and data item

$$P(p) = C(p)D(p) \tag{2}$$

where $C(\cdot)$ is the confidence item. The initial values of $C(\cdot)$ for the known pixels are 1s and for the unknown pixels are 0s. The confidence item of exemplar Ψ_p is

$$C(p) = \frac{\sum_{q \in \Psi_p \cap (\Omega - D)} C(q)}{|\Psi_p|} \tag{3}$$

where $|\Psi_p|$ is the size of exemplar, q denotes the pixel in exemplar. The more known pixels, the larger $C(p)$. $D(p)$ is the data item. The absolute value of cross-isophote diffusion TV is used as the data item [21]. Constrained by the cross-isophote diffused TV, the exemplar which is along linear structure has a high filling priority, and the linear structure is preserved. The equation of TV for a pixel in the image is

$$\begin{aligned} I(\xi)_t &= \nabla \cdot \left(\frac{\nabla I(\xi)}{|\nabla I(\xi)|} \right) = \frac{1}{|\nabla I(\xi)|} I(\xi)_{\bar{t}\bar{t}} \\ I(\xi)_{\bar{t}\bar{t}} &= \frac{I(\xi)_x^2 I(\xi)_{yy} + I(\xi)_y^2 I(\xi)_{xx} - 2I(\xi)_x I(\xi)_y I(\xi)_{xy}}{|\nabla I(\xi)|^2} \end{aligned} \tag{4}$$

where $I(\xi)_{\bar{t}\bar{t}}$ is the second order directional derivative along isophote for the color information of ξ, $\nabla \cdot$ is divergence operator, x, y are space reference frame. $I(\xi)$ along isophote is denoted as $I(\xi) \equiv \lambda$, ds denotes the length element along isophote, then

$$d\lambda/ds = |\nabla I(\xi)| \tag{5}$$

where $|\nabla I(\xi)|$ is the change of linear structure cross isophotes. The diffusion of TV in Eq. (4) depends on the contrast between isophotes, and it considers the extent of edge. The value of $1/|\nabla I(\xi)|$ is positive, but the sign of $I(\xi)_{\vec{t}\vec{t}}$ is determined by the region property at different sides of edges. $D(p)$ represents the data item of exemplar Ψ_p. It is used to determine the filling order, so it should be positive, and the diffusion with a negative $I(\xi)_{\vec{t}\vec{t}}$ can not be denoted with a low filling priority. So TV could not be used as the data item directly, and the absolute value form of it is used as the cross-isophote diffused data item. The data item of exemplar Ψ_p is computed as

$$D(p) = |I_{pt}| = \frac{|I_{p\vec{t}\vec{t}}|}{|\nabla I_p|} \tag{6}$$

where I_p is the color information in the exemplar Ψ_p. If $|\nabla I_p|$ is large, there is no isophote in this region and no linear structure in Ψ_p; $D(p)$ is small and the filling priority of Ψ_p is low. If $|\nabla I_p|$ is small, difference between isophotes is small, and Ψ_p lies along an isophote. To preserve the linear structure, the filling priority of Ψ_p is high.

The data item is an along-isophote diffused PDE in [17]

$$\begin{aligned} D(p) &= \frac{|\nabla I_p^{\perp} \bullet n_p|}{\alpha} \\ \nabla I_p{}^{\perp} &= \frac{\bar{N}_p}{|\bar{N}_p|} = \frac{(-I_{py}, I_{px})}{\sqrt{(I_{px})^2 + (I_{py})^2}} \end{aligned} \tag{7}$$

where $\nabla I_p^{\perp}$ is the isophote direction, n_p is the value of gradient normal to the target region contour direction ($\partial\Omega$). Along-isophote diffusion PDE does not consider the difference between isophotes. When different linear structures exist in the known parts of image, they will be propagated into the target region simultaneously and conflict with each other. Eq. (7) is just the absolute value form of the pure transportation image inpainting PDE proposed in [1] and $\nabla I_p^{\perp}$ is the transportation direction used in this model. The problem of conflicting diffusion does exist the in pure transportation model. In reference [1], this problem is solved by adding another anisotropic diffusion PDE during the transporting procedure. While used as data item, there is no diffusion in the cross-isophote direction in Eq. (7). So completed by the exemplar-based model in [17], some error texture patterns would be restored. As the analysis above, the cross-isophote diffusion PDE considers the extent of edges, and it is determined by the contrast between isophotes. So it has no problem of conflicting diffusion as the data item used in [17].

The linear structure preserving properties of different exemplar-based models are shown in Fig. 3. The target region is selected randomly in Fig. 3 (b), and this is different from the testing image in [17] which is a regular semicircle. Figs. 3 (c1)-(g1) is the filling procedure of the model which uses onion-peel order [11]. It fills the region from outside to inside, then artifacts are produced and linear structure is not preserved. Figs. 3 (c2)-(g2) are the filling procedure of the model in [17]. It fills the line firstly to preserve it. But it fills some isotropic region prior to parts of the line, so Fig. 3 (g2) is not as good

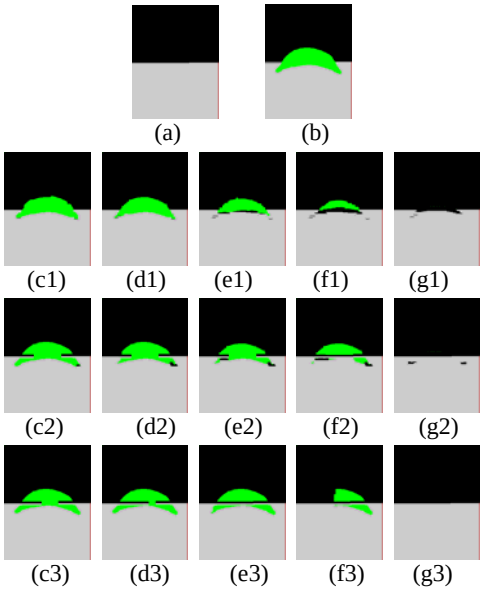

Fig. 3. Images processed by different exemplar-based completion methods. (a) Original image; (b) Image with target region; (c1)-(g1), (c2)-(g2), (c3)-(g3) Show completion procedure of onion-peel order model, the model in [17], the model proposed in this paper respectively.

as Fig. 3 (g3). Figs. 3 (c3)-(g3) show images processed by our model. It is clear it fills the line prior to other parts, so the linear structure is preserved well and no artifact is produced. The novel exemplar-based model whose filling order is constrained by cross-iso- phote diffusion PDE is more suitable for geometrical image completion.

2.4 Computing Similarity

When the filling order of exemplar is determined, the most similar source exemplar should be found. The color distance is used to weigh the difference between exemplars. The similarity function based on the color information is

$$\boldsymbol{\Psi}_{c\bar{q}} = \arg\min_{\boldsymbol{\Psi}_q \in \Omega - D} d_c(\boldsymbol{\Psi}_{\bar{p}}, \boldsymbol{\Psi}_q) \tag{8}$$

where $\boldsymbol{\Psi}_q$ is the source exemplar in the known parts of image $\Omega - D$, $\boldsymbol{\Psi}_{\bar{p}}$ is the partly completed exemplar in the target region, $d_c(\boldsymbol{\Psi}_{\bar{p}}, \boldsymbol{\Psi}_q)$ is the color distance between the known pixels in two exemplars, $\boldsymbol{\Psi}_{c\bar{q}}$ is the most similar exemplar which is chosen to fill into the target region. The exemplar in the known parts of image which has a least color distance with the exemplar in the target region is computed to be the chosen exemplar $\boldsymbol{\Psi}_{c\bar{q}}$. In this paper, the color distance is computed in the CIELAB color space, and the color distance $d_c(\bullet)$ is weighed by pixels' distances

$$d_c(\boldsymbol{\Psi}_{\bar{p}}, \boldsymbol{\Psi}_q) = \sum_{p_1 \in \boldsymbol{\Psi}_{\bar{p}}, p_2 \in \boldsymbol{\Psi}_q} L(p_1, p_2) \tag{9}$$

where p_1, p_2 are pixels in $\mathbf{\Psi}_{\bar{p}}, \mathbf{\Psi}_q$ respectively. In conventional exemplar-based model, only the color distance between exemplars is used to compute the similarity [11, 17]. For the non-textured image, if the color distance is small, the two exemplars are similar. When there are complex texture patterns in image, color similarity function is not enough, since the filled source exemplar should have a proper texture pattern. In this situation, the geometrical information should be adopted to weigh the similarity between exemplars. In this paper, the gradient information is incorporated and the gradient similarity function is

$$\mathbf{\Psi}_{g\bar{q}} = \sum \arg\min_{\mathbf{\Psi}_q \in \Omega - D} d_g(\mathbf{\Psi}_{\bar{p}}, \mathbf{\Psi}_q) \tag{10}$$

where $\mathbf{\Psi}_{g\bar{q}}$ is the exemplar which is most similar to the exemplar in the target region based on the known gradient information, $d_g(\bullet)$ is weighed by pixels' gradient information distance.. The selected exemplar $\mathbf{\Psi}_{g\bar{q}}$ contains similar gradient information to $\mathbf{\Psi}_{\bar{p}}$ in the target region, so the textured property is preserved.

The fusion method is introduced to derive the final composite similarity function

$$\mathbf{\Psi}_{\bar{q}} = \sum \arg\min_{\Psi_q \in \Omega - D} (\alpha d_c(\mathbf{\Psi}_{\bar{p}}, \mathbf{\Psi}_q) \oplus \beta d_g(\mathbf{\Psi}_{\bar{p}}, \mathbf{\Psi}_q)) \tag{11}$$

where $\oplus$ is a fusion operator, α and β are two fusion factors. Here we just choose a simple fusion method: $\oplus$ is chosen as a plus operator and $\alpha = \beta = 1/2$, $\mathbf{\Psi}_{\bar{q}}$ is the most similar source exemplar. The exemplar which has the least distance based on both the color and gradient information is the most similar one to the exemplar in target region.

The composite similarity function is suitable for the textured image. If the image is smooth, using the composite function may generate some error texture patterns and the conventional color similarity function is more suitable. Experimental results in next section will prove the validity of color similarity function and composite similarity function used in different images.

When the selected source exemplar is copied into the target region, the confidence item should be updated since more pixels are known

$$C(p) = C(\bar{p}), \ \forall p \in \mathbf{\Psi}_{\bar{p}} \cap \mathbf{\Omega} - D. \tag{12}$$

2.5 Removing Seams

The exemplar-based model processes image much faster than the single-pixel based model [8], but there are seams between exemplars. In this paper, a divergence constrained PDE is used to remove seams, and the PDE is derived following the basic conception of Poisson editing in [22]. The PDE Membrane Interpolation is

$$\min_{I(\xi)} \iint_{\mathbf{\Psi}_{\bar{q}}} |\nabla I(\xi)|^2 \ \text{ s.t. } J(\xi)|_{\mathbf{\Psi}_p} = I(\xi)|_{\mathbf{\Psi}_{\bar{q}}} \tag{13}$$

where $I(\xi)$ denotes the color value of pixel in the most similar source $\mathbf{\Psi}_{\bar{q}}$ generated by Eq. (11). These values are different from the original values in $\mathbf{\Psi}_{\bar{q}}$ and they are the constrained results of the Poisson equation. $J(\xi)$ is the existing value of the known pixel in

Ψ_p. The boundary condition of the Poisson equation is that the filled values in $\Psi_{\bar{q}}$ should be consistent with the existing values in Ψ_p. It is proved image processing in TV domain preserves the geometrical structure [21], so Eq. (13) is implemented in TV domain as

$$\min_{I(\xi)} \iint_{\Psi_{\bar{q}}} |\nabla I(\xi)| \text{ s.t. } J(\xi)|_{\Psi_p} = I(\xi)|_{\Psi_{\bar{q}}} . \tag{14}$$

The optimization procedure of it is

$$\nabla \cdot (\frac{\nabla I(\xi)}{|\nabla I(\xi)|}) = 0 \text{ s.t. } J(\xi)|_{\Psi_p} = I(\xi)|_{\Psi_{\bar{q}}} . \tag{15}$$

The overlapping exemplar interpolation is different from the simple image interpolation. There is filled information in Ψ_p, that is $J(\xi)|_{\Psi_p} = I(\xi)|_{\Psi_{\bar{q}}}$. So the interpolation procedure is constrained by the known information. For the simplicity of implementation, the Poisson Eq. (15) is written in guidance filed form

$$\min_{I(\xi)} \iint_{\Psi_{\bar{q}}} |\nabla \hat{I}(\xi)| \text{ s.t. } I(\xi) - J(\xi)|_{\Psi_p} = \hat{I}(\xi)|_{\Psi_{\bar{q}}} \tag{16}$$

where $\hat{I}$ is the overlapping information. In Eq. (16), the divergence value between two exemplars is minimized. And this value is computed under the constraint of the original value in Ψ_p. When the exemplar is copied into the target region, the removing seams process is executed to maintain the fusion between exemplar and its adjacent pixels. After this process, seams between color change and texture no longer exist.

2.6 Numerical Scheme

The processing result of PDE is affected by the numerical scheme. The cross-isophote data item which is used to determine the filling order is the result of a divergence operator. The numerical form of it is

$$D(p) = |I_{pt}| = |\nabla \cdot (\frac{\nabla I_p}{|\nabla I_p|})|. \tag{17}$$

If a simple central difference scheme is used to implement the data item, the divergence operator should be split firstly:

$$\nabla \cdot \mathbf{v} = \frac{\partial v^1}{\partial x} + \frac{\partial v^2}{\partial y},\ v^1 = \frac{I_{px}}{|\nabla I_p|},\ v^2 = \frac{I_{py}}{|\nabla I_p|}. \tag{18}$$

Take one direction in Fig. 4 as an example. To get the difference value of pixel O, I_{px}, I_{py}, ∇I_p are decomposed using the central difference scheme for pixel E respectively

$$v_E^1 = \frac{1}{|\nabla I(p)_E|}[\frac{\partial I_p}{\partial x}]_E \simeq \frac{1}{|\nabla I_{pE}|}\frac{I_{pX} - I_{pO}}{h} = \frac{I_{pX} - I_{pO}}{\sqrt{(I_{pX} - I_{pO})^2 + (I_{pNE} - I_{pSE})^2}}. \tag{19}$$

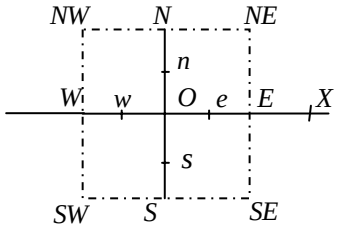

Fig. 4. Half-point difference structure.

The color information in pixel X is used to compute the difference value of pixel O. This operation exceeds the local adjacent domain in image processing [21]. While if the half-point difference scheme is executed, there is

$$v_e^1 = \frac{1}{|\nabla I_{pe}|}\left[\frac{\partial I_p}{\partial x}\right]_e \simeq \frac{1}{|\nabla I_{pe}|}\frac{I_{pE} - I_{pO}}{h} = \frac{I_{pE} - I_{pO}}{\sqrt{(I_{pE} - I_{pO})^2 + (I_{pNE} - I_{pSE})^2}}. \tag{20}$$

In Eq. (20), the difference operation of pixel e is executed within the 9-adjacent local domain. As analyzed in reference [21], if the difference operation exceeds the 9-adjacent local domain, the result of difference would not be precise. If the simple central difference scheme is used to compute the data item, the completed result of our model would contain some error filled texture patterns in the target region. This is because the pixel's matching domain is too large. So the half-point difference scheme is suitable for our model. The validity of the half-point numerical difference scheme is proved experimentally in next section.

3. EXPERIMENTS

The novel exemplar-based model is applied in different kinds of image to prove its validity in this section. The purpose of image completion is to restore the target region while satisfying the visual perception. The experimental results demonstrate that images generated by our model have satisfactory results.

Firstly, the experiment is given to prove that the selected target region greatly impacts the completed result. Figs. 5 (a1)-(a3) all contain a linear structure. Different target regions are selected in Figs. 5 (b1)-(b3), so the linear structures in three images are occluded by different target regions. Figs. 5 (c1)-(c3) are images completed by the model in [17]. They are the results of the same model, but they are thoroughly different. Figs. 5 (d1)-(d3) are the completed results of our model. Since our model has a good linear structure preserving property, it restores the linear structure under different situations.

The example in Fig. 6 demonstrates the advantage of the dynamic size of exemplar and the composite similarity function. Fig. 6 (a) is the original image and Fig. 6 (b) contains the selected target region. Fig. 6 (c) is the completed image using the exemplar-based model in [17]. In this image, there are many error texture patterns filled in the target region and the visual perception of it is bad. Fig. 6 (d) is the image generated by our model. The size of exemplar is dynamic determined and the gradient information affects

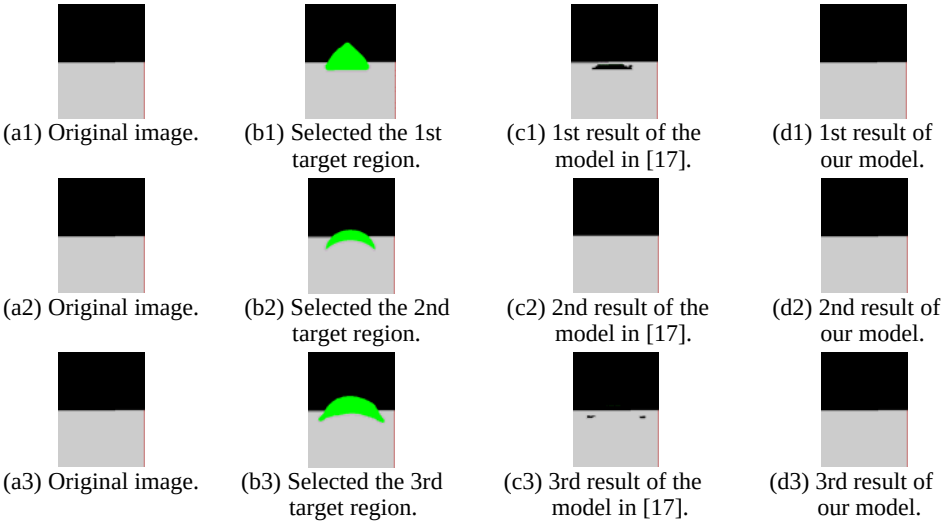

(a1) Original image. (b1) Selected the 1st target region. (c1) 1st result of the model in [17]. (d1) 1st result of our model.

(a2) Original image. (b2) Selected the 2nd target region. (c2) 2nd result of the model in [17]. (d2) 2nd result of our model.

(a3) Original image. (b3) Selected the 3rd target region. (c3) 3rd result of the model in [17]. (d3) 3rd result of our model.

Fig. 5. The completed results of one image with different target regions.

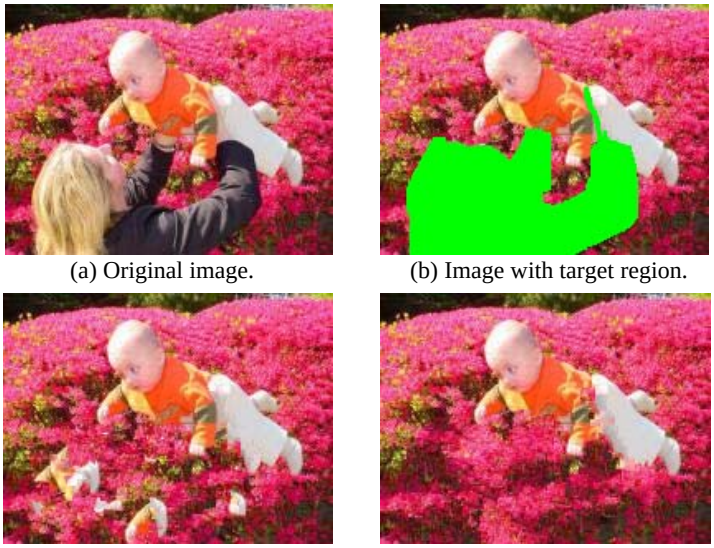

(a) Original image. (b) Image with target region.

(c) Result of the model in [17]. (d) Result of our model.

Fig. 6. Texture pattern completed results of different models.

the similarity between exemplars. The visual perception of Fig. 6 (d) is better than that of Fig. 6 (c), since gradient information is considered to generate Fig. 6 (d), and the texture patterns with different sizes are all preserved.

The linear structure preserving property of our model is further proved then. Figs. 7 (a) and (b) are original image and the image with a selected target region, respectively. Fig. 7 (c) is the completed result of the model in [17]. It is consistent with the completed result in [17]. The model proposed in [17] uses the exemplar with a single size and the

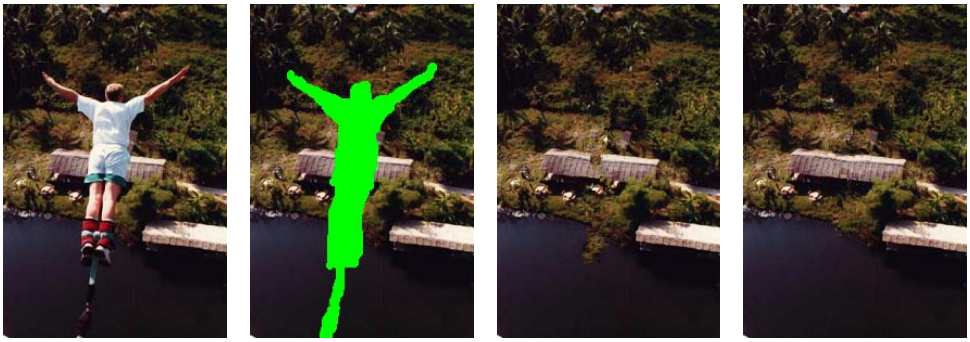

(a) Original image. (b) Image with target region. (c) Completed result of model in [17]. (d) Completed result of our model.

Fig. 7. The jumping image completion using exemplar-based model.

(a) Original image. (b) Result by using composite similarity function. (c) Result by using color similarity function.

Fig. 8. Completed result of different similarity function in our model.

filling order is constrained by along-isophote diffusion PDE. The riverbank in Fig. 7 (c) is propagated into the leg part of target region, and the linear structure of roof which is filled with leaves is breached. The completed result is not authentic. Fig. 7 (d) is the result of our model. In this image, the riverbank is completed with a plausible riverside, and the structure of roof is preserved. The visual perception of the image processed by our model is better, because the roof is never built with parts of leaves and the riverbank hardly has a suddenly extrusive part as that in Fig. 7 (c).

In the experiments of Fig. 7, just the color similarity function is used in our model. Only the color information is used to weigh the similarity between exemplars. This is because the task in this experiment is preserving the linear structures, and there are not many texture patterns. While in Fig. 6 different texture patterns should be filled and the similarity function is determined by both the color and gradient information. The image in Fig. 8 (b) is completed by our model which uses the composite similarity function, and there are error filled texture patterns. Fig. 8 (c) is just the image in Fig. 7 (d), and it is the result of our model using the color similarity function. The visual perception of Fig. 8 (c) is better than Fig. 8 (b). So it can be concluded that the composite similarity function is

suitable for textured image. For geometric image, traditional similarity function which is determined by the color information generates a better completed result.

The seams removing property of our model is proved in Fig. 9. The airplane in Fig. 9 (a) is to be removed. The contour of the airplane is left in Fig. 9 (c) which is the completed result of the model in [17]. The complete result of our model in Fig. 9 (d) is seamless. So the visual perception of the image processed by our model is better than that of the model in [17].

Images in Fig. 10 show the completion results of our model using different numerical schemes. Fig. 10 (a) is the testing image in Fig. 7. Fig. 10 (c) is just the completed image in Fig. 7 (d). It is generated by our model which uses the half-point numerical difference scheme. If the model uses the central difference scheme, processed result is just the image in Fig. 10 (b). There are error texture patterns filled in the roof and tree leaves. This is because the difference domain is too large. The completed results in Fig. 10 prove the benefit of the half-point difference scheme for divergence operator.

(a) Original image. (b) Image with target region. (c) Completed result of model in [17]. (d) Completed result of our model.

Fig. 9. Seamless completed result of exemplar-based model for image sky.

(a) Original image. (b) Completed result using central difference scheme. (c) Completed result using half-point difference scheme.

Fig. 10. Completed results using different difference schemes;

Exemplar-based model fills the target region using the source exemplars in the known parts of image. If there is no similar source exemplar, the visual perception of the completed image is bad. Fig. 11 (a) is a part of an image. In Fig. 11 (b) people in the background are selected to be removed. There is little image information about sky and beach. Image completed by the model in [17] is shown in Fig. 11 (c). The visual perception of it is bad, since there are many error filled texture patterns. The result of our model

(a) Original image. (b) Image with target region. (c) Completed result of model in [17]. (d) Completed result of our model.

Fig. 11. Completed result of our model in the image with little texture information.

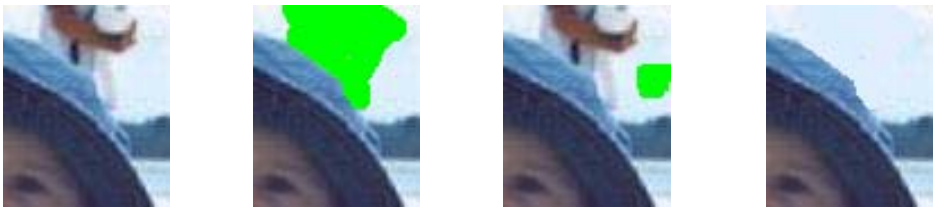

(a) Original image. (b) Image with target region. (c) Image with prescribed texture pattern. (d) Completed result of the extended model.

Fig. 12. Part of the completed image used extended model.

is in Fig. 11 (d); this image is not very good either. Edges of the baby's hat are not preserved. While we still can say that even in this situation, image completed by our model is better than that completed by the model in [17].

Lastly, we give an extended exemplar-based completion model to restore image with a prescribed texture pattern. Fig. 12 (a) is part of Fig. 11, and the target region is selected in Fig. 12 (b). From the experimental results in Fig. 11 it is concluded the image needs to be restored by a single kind of texture pattern. We extend the similarity function as

$$\begin{aligned} d'(\boldsymbol{\Psi}_{\bar{p}}, \boldsymbol{\Psi}_q) &= \sum_{\mathbf{s}\in\boldsymbol{\Psi}_{\bar{p}}, \mathbf{t}\in\boldsymbol{\Psi}_q} d(\mathbf{s},\mathbf{t}) + \sum_{\mathbf{s}\in\boldsymbol{\Psi}_{\bar{p}}, \mathbf{x}\in\boldsymbol{\Psi}_x} d^o(\mathbf{s},\mathbf{x}) \\ \boldsymbol{\Psi}'_{\bar{q}} &= \arg\min_{\boldsymbol{\Psi}_q\in\Phi} d'(\boldsymbol{\Psi}_{\bar{p}}, \boldsymbol{\Psi}_q) \end{aligned} \tag{21}$$

where $\boldsymbol{\Psi}_x$ is the prescribed texture pattern, x is the pixel in $\boldsymbol{\Psi}_x$, $d^o(\mathbf{s}, \mathbf{x})$ is the distance between pixels in un-processed exemplar and the exemplar in prescribed image, $d'(\boldsymbol{\Psi}_{\bar{p}}, \boldsymbol{\Psi}_q)$ is the distance between two exemplars. The similarity between exemplar and the texture pattern in prescribed image affects the selection of "filled-in" exemplar. Using Eq. (21), the target region is completed as the prescribed texture pattern. In Fig. 12 (c), color of the prescribed texture pattern is green, and Fig. 12 (d) is the image completed by the extended model. The edges in baby's hat are preserved well, and the background is properly restored.

4. CONCLUSIONS

In this paper a novel exemplar-based image completion model is proposed. The novel model uses a dynamic size of exemplar, and then proper exemplar could be found to fill in the target region. Exemplars along linear structure have large PDE constrained data items. These exemplars have higher filling priorities and are restored prior to other exemplars. When there are different kinds of texture pattern, no error texture information is filled into target region. For textured image, the similarity function is determined by both the color and gradient information, and then proper textureness exemplar is found. At last a divergence constrained PDE interpolation model is executed in the target region to remove seams between exemplars. Completed result is a smooth image.

In the last experiment, an extended exemplar-based model is used. Processed by this model, the target region is completed as a prescribed texture pattern. This operation is also called image analogies or image quilting [11, 23]. The usage of our model in image analogies is under research and we will refer to it in further papers.

REFERENCES

1. M. Bertalmio, G. Sapiro, V. Caselles, and C. Ballester, "Image inpainting," in *Proceedings of ACM SIGGRAPH Conference on Computer Graphics*, 2000, pp. 417-424.
2. T. F. Chan and J. Shen, "Morphologically invariant PDE inpaintings," Technical Report CAM 2001-15, Department of Mathematics, University of California Los Angeles, 2001.
3. M. Bertalmio, A. L. Bertozi, and G. Sapiro, "Navier-stokes, fluid dynamics and image and video inpainting," in *Proceedings of IEEE Conference on Computer Vision and Pattern Recognition*, 2001, pp. 355-362.
4. M. Bertalmio, "Strong-continuation, contrast-invariant inpainting with a third-order optimal PDE," *IEEE Transactions on Image Processing*, Vol. 15, 2006, pp. 1934-1938.
5. T. F. Chan and J. Shen, "Mathematical models for local nontexture inpaintings," *SIAM Journal on Applied Math*, Vol. 62, 2001, pp. 1019-1043.
6. M. Tran and A. Datta, "Synthesising textures using variable neighborhood searching," in *Proceedings of the 7th International Conference on Digital Image Computing-Techniques and Applications*, 2003, pp. 643-652.
7. T. Y. Ng, C. Wen, T. S. Tan, X. Zhang, and Y. J. Kim, "Generating an ω-tile set for texture synthesis," in *Proceedings of the 23rd Computer Graphics International*, 2005, pp. 177-184.
8. A. A. Efros and T. K. Leung, "Texture synthesis by nonparametric sampling," in *Proceedings of International Conference on Computer Vision*, 1999, pp. 1033-1038.
9. L. Y. Wei and M. Levoy, "Fast texture synthesis using tree-structured vector quantization," in *Proceedings of ACM SIGGRAPH Conference on Computer Graphics*, 2000, pp. 479-488.
10. S. C. Pei, Y. C. Zeng, and C. H. Chang, "Visual restoration of ancient Chinese painting using color contrast enhancement and lacuna texture synthesis," *IEEE Transactions on Image Processing*, Vol. 13, pp. 416-429.

11. A. A. Efros and W. F. Freeman, "Image quilting for texture synthesis and transfer," in *Proceedings of ACM Conference in Computer Graphics*, 2001, pp. 341-346.
12. R. Bornard, E. Lecan, L. Laborelli, and J. H. Chenot, "Missing data correction in still images and image sequences," in *Proceedings of ACM Multimedia*, 2002, pp. 355-361.
13. P. Perez, M. Gangnet, and A. Blake, "PatchWorks: Example-based region tiling for image editing," Microsoft Research Report MSR-TR-2004-04, 2004.
14. P. Harrison, "A non-hierarchical procedure for re-synthesis of complex textures," in *Proceedings of International Conference in Central Europe Computer Graphics and Visualization*, 2001, pp. 190-197.
15. I. Drori, D. Cohen-Or, and H. Yeshurun, "Fragment-based image completion," *ACM Transactions on Graphics*, Vol. 22, 2003, pp. 303-312.
16. J. Sun, L. Yuan, J. Jia, and H. Y. Shum, "Image completion with structure propagation," *ACM Transactions on Graphic*, Vol. 24, 2005, pp. 861-868.
17. A. Criminisi, P. Perez, and K. Toyama, "Region filling and object removal by exemplar-based image inpainting," *IEEE Transactions on Image Processing*, Vol. 13, 2004, pp. 1200-1212.
18. J. Y. Wu and Q. Q. Ruan, "Object removal by cross isophotes exemplar-based inpainting," in *Proceedings of the 18th International Conference on Pattern Recognition*, Vol. 3, 2006, pp. 810-813.
19. J. Y. Wu and Q. Q. Ruan, "A PDE constraint adaptive exemplar based image inpainting model," *Journal of Computer Aided Design and Computer Graphics*, Vol. 19, 2007, pp. 1034-1040.
20. C. Wang, Y. Du, and J. Du, "Research and application of image inpainting based on missing image blocks," *Computer Engineering*, Vol. 32, 2006, pp. 206-208.
21. T. F. Chan, S. Osher, and J. Shen, "The digital TV filter and nonlinear denoising," *IEEE Transactions on Image Processing*, Vol. 10, 2001, pp. 231-241.
22. P. Perez, M. Gangnet, and A. Blake, "Poisson image editing," *ACM Transactions on Graphics*, Vol. 22, 2003, pp. 313-318.
23. A. Hertz, C. E. Jacobs, N. Oliver, B. Curless, and D. H. Salesin, "Image analogies," in *Proceedings of ACM SIGGRAPH Conference on Computer Graphics*, 2001, pp. 327-340.

Ji-Ying Wu (仵冀穎) received the B.S. degree in Computer Science and Technology from Beijing Jiaotong University, Beijing, China in 2004. She is currently pursuing the Ph.D. degree at the Institute of Information Science (IIS), Beijing Jiaotong University. Her research interests are in computer vision, image denoising based on partial differential equation, image inpainting, object region removal.

Qiu-Qi Ruan (阮秋琦) received the B.S. and M.S. degrees from Beijing Jiaotong University, China in 1969 and 1981 respectively. From January 1987 to May 1990, he was a visiting scholar in the University of Pittsburgh, and the University of Cincinnati. Subsequently, he has been a visiting professor in USA for several times. He has published 4 books and more than 100 papers, and achieved a national patent. Now he is a professor, doctorate supervisor and the head of the institute of information science, Beijing Jiaotong University. He is a senior member of IEEE. His main research interests include digital signal processing, computer vision, pattern recognition, and virtual reality *etc.*